Two-Dimensional Ordered Arrays of Silica Nanoparticles

Ce Wang,*,† Yahong Zhang,† Lin Dong,† Limin Fu,† Yubai Bai,† Tiejin Li,† Jigeng Xu,‡ and Yen Wei*,‡

Departments of Chemistry, Jilin University, Changchun, 130023, P. R. China, and Drexel University, Philadelphia, Pennsylvania 19104

Received November 23, 1999. Revised Manuscript Received July 25, 2000

Nanosized silica particles of various diameters (40, 60, and 105 nm) with relatively narrow size distributions were prepared via base-catalyzed sol−gel reactions of tetraethyl orthosilicate using a seeded-growth technique. These nanoparticles were organized into two-dimensional (2-D) monolayers by a solvent evaporation method. The particles of 60 nm or greater in diameter could be assembled to 2-D crystals on a larger area because of lower particle size distribution. The arraying order was found to have little or no dependence on shape regularity of the nanoparticles, pH value, and type of the substrate, including microslide, silicon wafer, and indium−tin oxide glass, used in this study.

Introduction

Optical properties of green compacts of silica colloids are known to depend on microstructure parameters, such as particle size that is between several nanometers and micrometers, size distribution, and spatial arrangement order of silica particles.[1−3] For self-assemblies of submicrometer-sized particles, high polydispersity (i.e., broad size distribution) leads to an amorphous structure that reduces reflectivity without sacrificing other optical qualities, and therefore, refractive indices can be adjusted by varying proportions of the particles with different sizes.[3,4] Under proper conditions, monodipersed particles can undergo orderly self-organization to form photonic crystals with a regular array in two- (2-D) or three-dimensions (3-D).[5] The refractive indices of such assemblies increase approximately linearly with the number of layers.[6] For nanosized particles of about 100 nm or lower in diameter, both amorphous and crystalline monolayers exhibit similar antireflection properties in the entire visible light spectrum and are potential planar waveguide materials in the ultraviolet regions.[7] However, many optical properties of 2-D ordered assemblies of the nanoparticles with diameters smaller than 100 nm are not yet fully understood, probably because of relatively few studies on the assembling techniques. In addition, it is much easier to buy or make monodispersed polystyrene particles than silica particles, and this along with the bigger refractive index of polystyrene is among the main reasons for the fact that the majority of the work in the field of nanoparticle assemblies is carried out on polystyrene.[8]

There have been several reports on the assembling of nanosized silica colloids.[7,9] For example, Iler succeeded in obtaining particle assembly by rubbing silica powders on clean glass surfaces using his fingertip in 1972.[9a] Böhmer et al have achieved the array by electrostatic adsorption of particles on a silicon wafer pretreated with poly(vinylimidazole).[9b] However, these monolayers exhibit a rather disordered structure. It is noted that, in many excellent works on 3-D assemblies of silica particles,[6,10] the surfaces of the compacts often exhibit high 2-D crystallinity.

There have been various techniques to fabricate 2-D photonic crystals of silica particles of 100−1000 nm in diameters. For instance, intense light fields have been used to organize the 2-D crystals by forcing particles with a higher refractive index than the solvent to crystallize on the intensity maxima of an interference pattern created by several laser beams.[11] An electrophoretic technique has been applied to sediment fine silica spheres to ordered monolayer.[10] The technique of air−liquid interface was applied to form a hexagonal-close-packed polycrystalline monolayer by using the silica particles coated with long chain alcohols[12] and could be transferred onto other solid surfaces.[13] Silica

* To whom correspondence should be addressed. E-mail: wjzhang@mail.jlu.edu.cn (C.W.); weiyen@drexel.edu (Y.W.).
† Jilin University.
‡ Drexel University.

(1) Lin, S. Y.; Chow, E.; Hietala, V.; Villeneuve, P. R.; Jonnopoulos, J. D. *Science* **1998**, *282*, 274.
(2) Kin, S. Y.; Fleming, J. G.; Hetherington, D. L.; Smith, B. K.; Biswas, R.; Ho, K. M.; Sigalas, M. M.; Zubrzycki, W.; Kurtz, S. R.; Bur, J. *Nature* **1998**, *394*, 251.
(3) Endo, Y.; Ono, M.; Yamada, T.; Kawamura, H.; Kobara, K. *Nyo Seramikkusu* **1995**, *8*, 31.
(4) Endo, Y.; Ono, M.; Yamada, T.; Kawamura, H.; Kobara, K.; Kawamura, T. *Funtal Kogaku Kaishi* **1995**, *32*, 170.
(5) (a) Mayoral, R.; Requena, J.; Moya, J. S.; López, C.; Cintas, A.; Míguez, H.; Meseguer, F.; Vázquez, L.; Holgado, M.; Blanco, À. *Adv. Mater.* **1997**, *9*, 257. (b) Russel, B.; Saville, D. A.; Schowalter, W. R. *Colloidal Dispersions*; Cambridge University Press: Cambridge, U.K., 1989. (c) Van Blaaderen, A.; Wiltaius, P. *Adv. Mater.* **1997**, *9*, 833.
(6) Jiang, P.; Bertone, J. F.; Hwang, K. S.; Colvin, V. L. *Chem. Mater.* **1999**, *11*, 2132.
(7) Dimitrov, A. S.; Miwa, T.; Nagayama, K. *Langmuir* **1999**, *15*, 5257.
(8) This sentence is a direct quotation from one of the reviewers of this work..
(9) (a) Iler, R. K. *J. Colloid Interface Sci.* **1972**, *38* (2), 496. (b) Böhmer, M. R.; van der Zeeuw, E. A.; Kope, G. J. M. *J. Colloid Interface Sci.* **1998**, *197*, 242. (c) Kondo, M.; Shinozaki, K.; Bergstrom L.; Mizutani, N. *Langmuir* **1995**, *11*, 394.
(10) Furuuchi, M.; Mori, S.; Gotoh, K. *Powder Technol.* **1994**, *80*, 159.
(11) Burns, M. M.; Fournier, J. M.; Golovchenko, J. A. *Science* **1990**, *249*, 749.
(12) Laible, R.; Hamann, K. *Adv. Colloid Interface Sci.* **1980**, *13*, 65.
(13) Kimizuka, N.; Fujikawa, S.; Kunitake, T. *Adv. Mater.* **1998**, *10*, 1373.

10.1021/cm990738j CCC: $19.00
Published on Web 11/22/2000

crystalline monolayers grown from water suspensions by forming a suspension wetting film on the glass surface and controlling the rate of the receding glass−suspension−air three-phase contact line have been reported.[6]

In this paper, we report the synthesis of silica nanosized particles of 40−105 nm in diameter with narrow size distributions by base-catalyzed hydrolysis and polycondensation (i.e., sol−gel reactions) of tetraethyl orthoslicate (TEOS) at room temperature. By importing the solvent evaporation method for assembling polymer latex nanospheres,[14] we have achieved 2-D ordered assembling of silica nanoparticles. One of the advantages of this method is that salt and surfactant are not required for the assembling of monolayers.[14] The silica nanoparticles and their 2-D assemblies are characterized by means of atomic force microscopy (AFM), scanning electron microscopy (SEM), and X-ray photoelectron spectroscopy (XPS). The order of 2-D arrays is examined in relations with various synthetic parameters such as shape regularity of the nanoparticles, pH value, and type of the substrate, including microslide, silicon wafer, and indium−tin oxide glass.

Experimental Section

Materials and Instrumentation. Tetraethyl orthosilicate (TEOS, CR) was purchased from the Third Reagent Factory of Shenyang (Shengyang, China) and purified by distillation under a reduced pressure before use. Ethanol (AR) and ammonia (NH_4OH, 25−28 wt %, AR) from the Tian Tai Reagent Factory (Tianjing, China) were used as received. The scanning electron microscopy (SEM) images were recorded with a Hitachi S-570 scanning electron microscope on the samples coated with gold by using an Ion Coater (Eiko, IB-3). Atomic force microscopy (AFM) images were obtained on a Park Scientific Instruments Autoprobe CP in noncontact mode in order to avoid possible destruction of the samples. The samples for SEM and AFM images were prepared by spreading 20 μL of the dilute suspension on the substrate and letting them stand overnight in the preparation box without disturbance. XPS was recorded with a VG ESCALAB MKII electronic energy spectrometer (VG Co., England).

Preparation of Silica Nanoparticles. Silica nanoparticles were prepared by base-catalyzed sol−gel reactions of TEOS using the seeded-growth technique similar to that in the literature.[15] In a typical nanoparticle preparation, 1.5 mL of TEOS, 1.7 mL of ammonia (25 wt %), 1.0 mL of deionized water, and 50 mL of ethanol were introduced into a 250-mL round-bottomed glass flask. After the mixture was stirred at 40 °C for 3 h, an additional 1.0 mL of TEOS was added into the system and the reactions were allow to continued for another 3 h. The system was then diluted several (e.g., 10) times with deionized water. Ethanol was removed from the system through a rotary-evaporator. By this process, a suspension containing colloidal particles of about 40 nm in diameter was obtained. In addition, similar colloidal silica particles with diameters of 60 and 105 nm were obtained when the amount of ammonia in the above reaction system was increased from 1.7 to 2.0 and 3.0 mL, respectively.

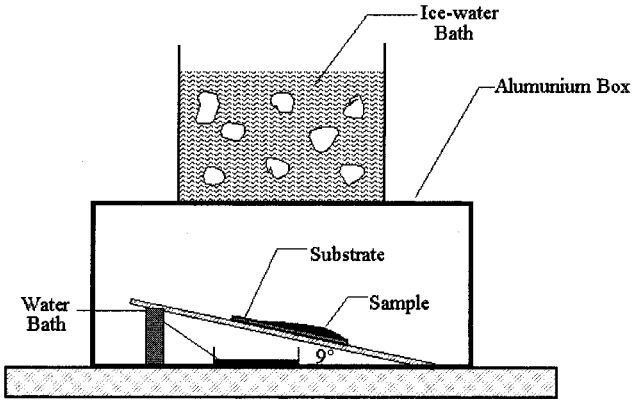

Figure 1. Schematic drawing of the evaporation system for assembling silica nanoparticles.

Treatment of Substrate Surface. Microslide, silicon wafer (n, 111), and ITO (indium−tin oxide) glass, after pretreatment of surfaces, were used as substrates for the nanoparticle assembling. The microslide and silica wafer were first cleaned in trichloroethane and then in a freshly prepared mixture of H_2SO_4 and H_2O_2 (30%) at a volume ratio of 4:1, followed by rinsing thoroughly with deionized water (16 MΩ·cm) and drying at room temperature. The ITO glass was first immersed in a saturated potassium hydroxide aqueous solution for about 10 h and then ultrasonically cleaned in deionized water for 10 min, followed by rinsing sequentially with acetone, ethanol, and deionized water. Finally, it was stored in 2-propanol before use.

Experimental Setup and Procedure. The experimental setup for nanoparticle assembling, as schematically shown in Figure 1, was adopted from that for assembling polymer latex nanospheres.[14] The aluminum container has a volume of about 50 cm^3. An ice−water bath was put onto the top of the aluminum box, and a water bath, under the substrate inside the box. The ice−water bath was used to cool the system for reducing the rate of water evaporation and for slowing down the Brownian motion of the particles. The water bath was to maintain a constant humidity in the evaporating system in order to reduce the rate of water evaporation and to keep a water film between the lateral sides of the particles. The useful preparation area on the substrate was about 1 × 1 cm^2.

The concentration of the silica particles in the suspension (ω, g/mL) may be calculated according to the following formula:

$$\omega = \frac{V_0 \rho_T M_2}{V_d M_1} \quad (1)$$

Here V_0, ρ_T, and M_1 are the total volume, density, and molecular weight of TEOS, respectively; M_2 is the molecular weight of silica, and V_d is the total volume of the suspension.

Moreover, another equation can be derived by simplifying the one described by Micheletto[15] covering an area of 1.0 cm^2:

$$\omega = \frac{2\rho\phi}{3v} \times 10^{-4} \quad (2)$$

Here ρ and ϕ are the density and diameter of silica particles and v is the volume of the suspension needed on the area of 1 cm^2. If we assume that the density of silica is 1.9 g/cm^3 (ρ)[16] and use 20 μL (v) of the suspension in the preparation, the above equation can be further simplified as

$$\omega = \frac{6\phi}{1000} \quad (3)$$

By substituting all the known parameters (e.g., V_0, ρ_T, M_1, M_2) in eq 1 and determining the particle diameter (ϕ) with

(14) Micheletto, R.; Fukuda, H.; Ohtsu, M. *Langmuir* **1995**, *11*, 3333 and references therein.

(15) (a) Konno, M.; Inomata, H.; Matsunaga, T.; Saito, S. *J. Chem. Eng. Jpn.* **1994**, *27* (1), 134. (b) Stöber, W.; Fink, A. *J. Colloid Interface Sci.* **1968**, *26*, 62. (c) Bogush, G. H.; Tracy, M. A.; Zukoski, C. F., IV. *J. Non-Cryst. Solids* **1988**, *104*, 95. (d) Bogush, G. H.; Zukoski, IV, C. F. *J. Colloid Interface Sci.* **1991**, *142*, 1. (e) van Blaaderen, A.; Geest, J. V.; Vrij, A. *J. Colloid Interface Sci.* **1992**, *154* (2), 483. (f) van Blaaderen, A.; Kentgens, A. P. M. *J. Non-Cryst. Solids* **1992**, *149*, 161. (g) Konno, M.; Inomata, H.; Matsunaga, T.; Saito, S. *J. Chem. Eng. Jpn.* **1994**, *27* (1), 134.

(16) Iler, R. K. *The Chemitry of Silica*; Wiley-Interscience: New York, 1979; pp 387−390.

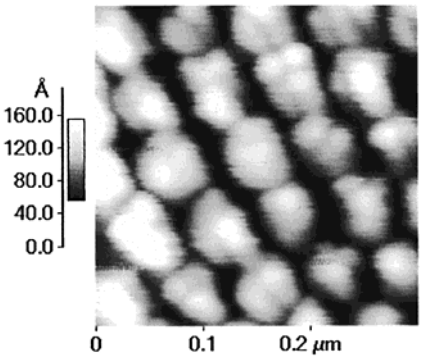

Figure 2. AFM image of 60-nm silica particles assembled as a monolayer on a microslide.

SEM, we could determine the total volume (V_d) of the suspension needed for each preparation, which was obtained by diluting the as-synthesized suspension of silica nanoparticles with deionized water.

Results

Preparation and Particle Size Distribution of Silica Nanoparticles. Using the seeded-growth technique, we have obtained silica nanoparticles with diameters of 40−100 nm by the base-catalyzed sol−gel process at room temperature. The particle size can be tuned simply by changing the amount of ammonia catalyst employed. XPS data indicate that the silica particles, at least on their surfaces, consist of ∼35 wt % silicon and ∼52 wt % oxygen, suggesting that the hydrolysis and polycondensation of TEOS were quite complete to afford silica. A small amount of nitrogen (∼0.2 wt %) observed in XPS could be attributed to ammonium ions that are attached to the surface of the silica with negative charges (i.e., $Si-O^-$) by electrostatic force at the medium acidity higher than the isoelectric point of pH 2 for silica nanoparticles.[16]

Figure 2 shows the AFM image of 60-nm silica particles. While the particles are quite regular in sizes, some of them appear to have substructures which might be resulted from aggregation of smaller subparticles.[15d] Similar irregularity of the particle shape was also observed for 40-nm silica. However, the 105-nm particles showed a nearly perfect spherical shape with little surface roughness in comparison with the 40- and 60-nm particles. A similar trend was also observed in the particle size distributions. By measurement of the diameters of 200 individual particles in the SEM micrographs (Figure 3), the particle size distributions were obtained as shown in Figure 4 for each of the 3 particle sizes. The size distribution clearly becomes narrower as the diameter of the silica particles is increased. From Figure 4a−c, polydispersity (PD) values as represented by percentages of standard deviations from the mean diameter of the particles are calculated to be 32, 13, and 4% for the 40-, 60-, and 105-nm particles, respectively.

Array of Silica Nanoparticles. Upon assembly by the solvent evaporation method, the 2-D monolayers of silica nanoparticles all exhibit good ordering as shown in Figure 3. The degree of ordering appears to depend mainly on the polydispersity (i.e., size distribution) of the particles. The 105-nm particles (PD = 4%) shows an very good hexagonal order (Figure 3c). The 60-nm particles (PD = 13%) also have regular hexagonal

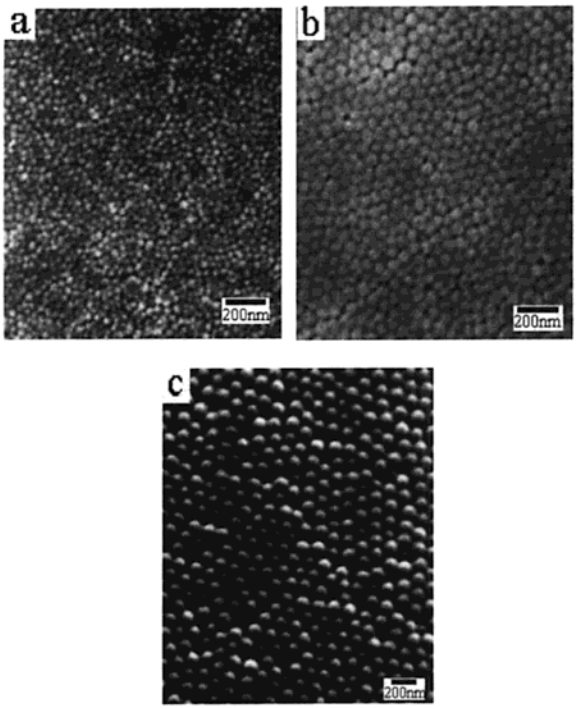

Figure 3. SEM images of the monolayers on a microslide for nanoparticles with diameters of (a) 40 nm, (b) 60 nm, and (c) 105 nm, assembled at pH 8.0.

arrangement (Figure 3b) though the ordered domain sizes are somewhat smaller than those for the 105-nm particles. In comparison, the degree of ordering in the 40-nm particle (PD = 32%) assembly is much lower (Figure 3a). All these monolayers of silica nanparticles were found quite stable without agglomeration, even after storage for a long period of time.

The coverage of the monolayers on the total deposition areas is reasonably good (∼75−85%) by the solvent evaporation method. Taking the sample prepared from the suspension of the particles of 60 nm in diameter as a typical example, the SEM image (Figure 5) shows that the assembly of the particles covered approximately 75% of the total deposition area (1 × 1 cm^2). The ordered monolayer of the particles was mainly located at the upper part of the substrate (Figure 5a) with domain size of several micrometers. Less ordered multilayers were found at the lower side of the substrate (Figure 5d). The uncovered surfaces are largely located in the central parts of the substrate in the forms of domains (Figure 5b) and strips with ca. 17−32 μm width (Figure 5c). The area of the monolayers could be enlarged as the temperature for assembling process was decreased, understandably because of the lowered rate of the Brownian motion of the particles.

Effect of pH on the Arraying. In the above-mentioned preparations, the monolayers were prepared by assembling the nanoparticles on the microslide at pH 8.0. To evaluate the effect of pH on the arraying of silica nanoparticles, the pH value of the suspension medium was changed from 8.0 to 1.0 for assembling the monolayer of 60-nm silica particles. The SEM images show that there is no appreciable difference in the ordering array of the particles assembled at various pH values.

Effect of Substrates on the Arraying. To examine the effect of smoothness of the substrate surfaces on the

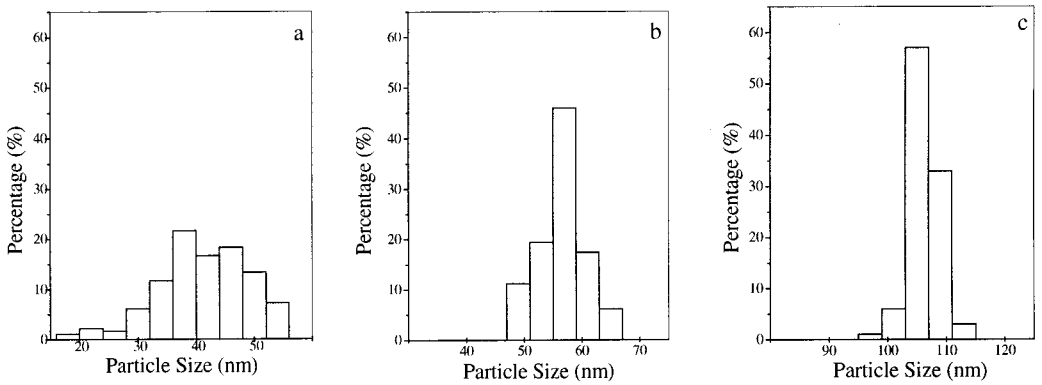

Figure 4. Particle size distributions of silica nanoparticles: (a) 40 nm; (b) 60 nm; (c) 105 nm.

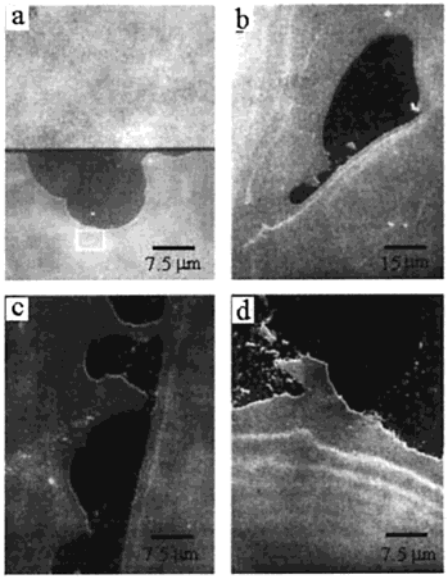

Figure 5. SEM images, taken in various sections, of a silica nanoparticle (60 nm) assembly on a microslide: (a) upper section of the microslide with a part enlarged; (b) middle section in a domain form; (c) middle section in a strip form; (d) lower section.

arraying of silica nanoparticles, AFM images of surfaces of the microslide, ITO glass and also silicon wafer were recorded. The microslide and ITO glass were found to have many strip structures and protruding points on the surfaces. The difference between the lowest and highest points was nearly 170 nm as shown, for example, in Figure 6a for the microslide. In contrast, the surface of silicon wafer was much smoother, and the difference was only ~2 nm in height (Figure 6b). As a consequence, the total area coverage of the assemblies on the silicon wafer (~85%) was greater than those on the slide and ITO glass (both ~75%). The appearance of the nanoparticle assembles on all of these substrates is similar to that shown in Figure 3 that was obtained on the microslides. These observations suggest that the success of attainment of ordered 2-D assemblies could be attributed to the hydrophilic substrate surfaces containing hydroxyl groups (OH) as generated by the chemical pretreatment of the surfaces[17] rather than to the physical features of the surfaces.

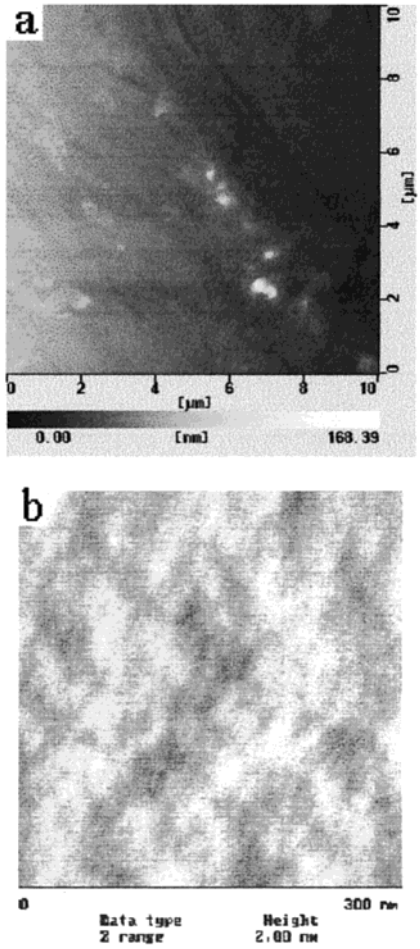

Figure 6. AFM images of the surfaces of (a) a microslide and (b) a silicon wafer.

Discussion

The mechanism of the crystalline monolayer formation by the similar solvent evaporation method has been discussed in many articles related to organic polymer latex spheres.[18−23] However, the negatively charged

(17) He, Y.; Thiry, P. A.; Yu, L. M.; Caudano, R. *Surf. Sci.* **1995**, *331−333*, 441.
(18) Rakers, S.; Chi, L. F.; Fuchs, H. *Langmuir* **1997**, *13*, 7121.
(19) Dimitrov A. S.; Nagayama K. *Langmuir* **1996**, *12*, 1303.
(20) Denkov, N. D.; Velev, O. D.; Kralchevsky, P. A.; Ivanov, T. B. *Langmuir* **1992**, *8*, 3183.
(21) Dimitrov, A. D.; Dustikin, C. D.; Yoshimura, H.; Nagayarna, K. *Langmuir* **1994**, *10*, 432.
(22) Hayashi, S.; Kumamoto, Y.; Suzuki, T.; Hirai, T. *J. Colloid Interface Sci.* **1991**, *144*, 538.
(23) Du, H.; Chen, P.; Liu, F. Q.; Meng, F. D.; Li, T. J.; Tang, X. Y. *Mater. Chem. Phys.* **1997**, *51* (3), 277.

surface of the silica naoparticles prepared in the presence of base catalyst is fundamentally different from that of polymer latex spheres. The self-organization of the silica particles is generally believed to be realized by combined effects of the following forces: capillary force; convection force; ionic attraction; hydrogen bond and electrostatic repulsion.[9,16,24]

Thus, the film formation starts when a very dilute suspension droplet contacts the hydrophilic substrate surface and the water film becomes as thin as the diameter of the particles. When the particles protrude out of the water surface, the meniscus formed between two neighboring particles results in strong capillary forces. The lateral capillary forces drag the particles together, leading to the formation of 2-D particle clusters. Once the silica particles are very close to each other, their interactions could be stronger because of ionic attraction force through the small amount of ammonium cations (as evidenced by our XPS results) that occupy the silica surface only at the points of contact between particles.[24] The particles far away from the ordered domains are transferred toward the already aggregated ones by the convection forces, which arise from water evaporation. In other words, the evaporation of water at the already existing aggregate site would cause a water flux carrying more particles toward the existing cluster. These approaching particles can attach themselves to the growing cluster only around its edge, where the electrostatic repulsion between the particles is least or the interaction force of the hydrogen bonds between the particles is strongest,[16] and, therefore a monolayer of particles is formed with good stability.

The degree of ordering is mainly dependent on the polydispersity of the nanoparticles. As expected, the lower the polydispersity the higher the degree of ordering as well as the larger the hexagonally packed particle domains.[6] The shape regularity of the particles appears not as important as polydispersity. The area of ordered array of the nanoparticles, unlike that of the submicrometer-sized photonic crystals,[5] is very sensitive to the evenness of substrate surfaces. A height difference of larger than 100 nm on the substrate surface could result in the disruption of the nanoparticle monolayers. A convex point may lead to the formation of a particle-free domain (Figure 5b), whereas convex along the strip structure on the substrate surfaces (Figure 6) may induce the occurrence of striplike uncovered areas (Figure 5c). Since the silicon wafer has a much smoother surface than the others, the area covered by nanoparticle assembly is larger.

The inhomogeneous spreading of the water film on the tilted substrate might contribute to the formation of multilayers on the bottom part of the substrate (Figure 5d). In general, the suspension film is thicker in the lower part of the substrates. When the thickness of the film is greater than the diameter of the particles, a multilayer rather than a monolayer is formed. Furthermore, during the process of arraying, the particles with about the same diameter preferentially form dense hexagonal packing and repulse those with smaller or larger particle sizes, due to the competing capillary forces among neighboring particles. Therefore, the array becomes disordered. In addition, water in the thinner films evaporates much faster than that in the thicker bottom part, so that the water film cracks more often in the middle region of the substrate surfaces. The rifts could be further amplified by unevenly distributed water−water and particle−particle interactions.

It is not difficult to understand that the acidity of the suspension did not affect the arraying order of the nanoparticles. The isoelectric point (IP) of silica particles[16] is pH 2. At pH values above IP, the particles are negatively charged (Si−O^-) and their interactions would be facilitated by cations such as ammonium in the system, while at pH ≤IP the hydroxyl groups (Si−OH) occupy the particle surfaces and hydrogen bonding should enhance the particle−particle interactions.[17] By the same token, the surfaces of the microslide, silicon wafer, and ITO glass are rich in OH groups after the chemical pretreatment. Therefore, the nanoparticles can all be arranged on the substrates by means of electrostatic attraction or hydrogen-bonding forces. Further investigation is in progress to evaluate effect of both the nature and concentration of additional salts on the nanoparticle assemblies.

Acknowledgment. This work was supported in part by the Chinese Natural Science Foundation Committee (Grant No. 59873009) and in part by the National Institutes of Health (Grant No. DE09848). We are most grateful to three reviewers whose suggestions have substantially improved the manuscript.

CM990738J

(24) Brinker, C. J.; Scherer, G. W. *Sol-Gel Science*; Academic Press: San Diego, CA, 1990; pp 241−294.